Installation of Spectrally-selective Imaging System in RF Negative Ion Source[a)]

K. Ikeda,[1] D. Wünderlich,[2] U. Fantz,[2] B. Heinemann,[2] M. Kisaki,[1] K. Nagaoka,[1] H. Nakano,[1] M. Osakabe,[1] K. Tsumori,[1] S. Geng,[3] O. Kaneko,[1] and Y. Takeiri[1]
[1)] *National Institute for Fusion Science, 322-6 Oroshi, Toki, Gifu, 509-5292, Japan*
[2)] *Max-Planck-Institut für Plasmaphysik, Boltzmannstraße 2, 85748 Garching, Germany*
[3)] *The Graduate University for Advanced Studies, 322-6 Oroshi, Toki 509-5292, Japan*

(Dated: 17 August 2015)

A spectrally-selective imaging system has been installed in the RF negative ion source in the ITER-relevant negative ion beam test facility ELISE to investigate distribution of hydrogen Balmer-α emission (H_α) close to the production surface of hydrogen negative ion. We selected a GigE vision camera coupled with an optical band-path filter, which can be controlled remotely used high speed network connection. A distribution of H_α emission near the bias plate has been clearly observed. The same time trend on H_α intensities measured by the imaging diagnostic and the optical emission spectroscopy is confirmed.

PACS numbers: 42.30.-d, 41.75.Cn

I. INTRODUCTION

A spectrally-selective imaging system has been developed and installed in the arc discharge type negative hydrogen ion (H^-) source in the National Institute for Fusion Science (NIFS)[1,2]. This system has been well performed to visualize a reduction in the distribution of hydrogen Balmer-α emission (H_α) owing to H^- ions; these findings have contributed to the high performance and safety operation for a neutral beam injector (NBI) in the Large Helical Device (LHD).

On the other hand, large scale H^- source based on RF discharge will be constructed for the NBI at the International Thermonuclear Experimental Reactor (ITER)[3]. Optimization of RF source performance and variable operation outputs have been carried out from a half size H^- source in ELISE test facility at Max-Planck-Institut für Plasmaphysik (IPP) Garching[4]. Current densities near the ITER NBI requirements have been achieved in hydrogen with low co-extracted electrons[5]. An optical emission spectroscopy (OES) diagnostic is kept running at ELISE operation to obtain plasma parameters and its homogeneity[6]. Distribution of H_α has a capability to obtain behavior of electrons and negative hydrogen ions in RF H^- source which is also important knowledge for production high power beam and optimization of beam shape.

In this paper, we present a configuration of a spectrally-selective imaging system based on a GigE vision camera for the ELISE RF hydrogen negative ion source. A clear high-resolution monochromatic image has been taken, and a value of distance per pixel of image is obtained by scale calibration. We will show the distribution image of H_α emission close to the bias plate surface in the typical RF discharge.

[a)] Contributed paper published as part of the Proceedings of the 16th International Conference on Ion Source, New York, USA, August, 2015.

II. CONFIGURATION OF SPECTRALLY-SELECTIVE IMAGING SYSTEM

Figure 1 shows the schematic drawing of the RF hydrogen negative ion source in ELISE. Hydrogen plasmas are generated in four cylindrical RF drivers by six-turn copper coils, and it expand into the extraction region near a plasma grid (PG) surface. A metal bias plate (BP) with eight opening windows around the beamlet groups covers the PG surface. Hydrogen negative ions are produced on cesiated metal surfaces and are extracted through the apertures. The 28 diagnostic ports (14 in horizontal and 14 in vertical) are positioned in the source at the upstream position to observed near the BP surface[6]. We set a spectrally-selective imaging system at the XR−1U port with the diameter of 40 mm quartz window. The line of sight (LOS) is arranged paralleled to the BP and PG surface with the distance of 7 mm and 20 mm, respectively, from the port center. The opposite side viewing port of XL−1U is used for optical emission spectroscopy (OES) to observe time trace of H_α, H_β, H_γ, and Cs spectrum in the source.

Figure 2 shows the system configuration of the spectrally-selective imaging system. We use a network connection CCD camera (AVT : MAKO G125B) based on the GigE vision standard. The type of charge-coupled device (CCD) detector (Sony : ICX445ALA) is a progressive black and white sensor which size is 1/3 inch. The effective chip size is 4.8 mm × 3.6 mm with the pixel

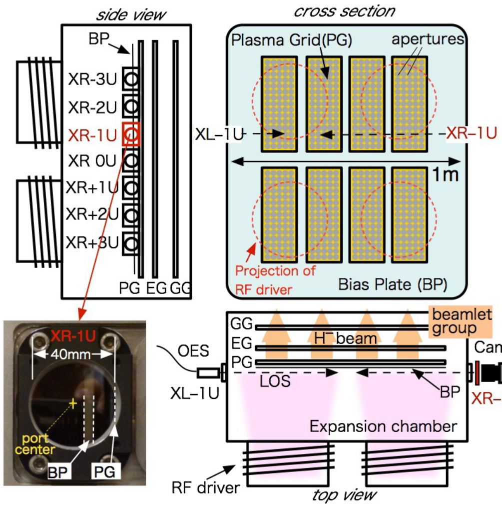

FIG. 1. Schematic cross-section drawing of RF hydrogen negative ion source for ELISE. The LOS for imaging diagnostic located on the XR−1U port is across extraction region near the BP surface. The OES diagnostics are set opposite side viewing ports XL−1U.

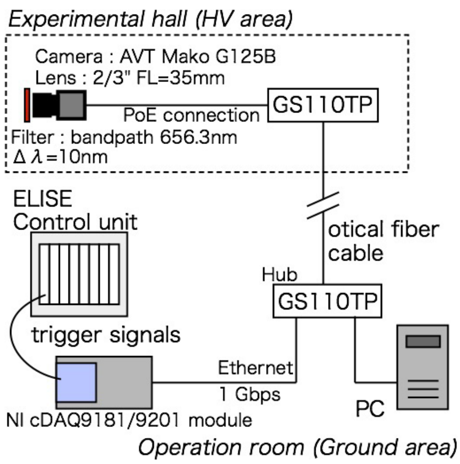

FIG. 2. Schematic diagram of the spectrally-selective imaging system. The CCD camera is mounted on the H$^-$ source of high-voltage state in the experimental hall for ELISE. That is controlled at the operation room used fast Ethernet network connection. Trigger signals are acquired by a compact DAQ system connected with same network.

resolution of 1292 × 964 pixels using a square cell of 3.75 μm. We use a 2/3 inch C-mount lens with focal length of 35 mm; the focal point is fixed 52 cm far from the lens where is the center of the ion source. An interference band path filter for H$_\alpha$ emission with the central wave length of 656.3 nm and 10 nm full width half maximum (FWHM) is inserted in front of the lens. The camera is driven by 12 V DC power suppled from a PoE (Power on Ethernet) hub (NETGEAR: GS110TP) located on a high voltage rack in the experimental hall. The CCD camera is remotely controlled from the operation room for ELISE using fast internal Ethernet network with optical fibers. An image in 12-bit monochrome is captured at timing of trigger signal detected by a compact DAQ system (NI: cDAQ9181 with 9201 module) connected with same network.

III. SPATIAL SCALE CALIBRATION AND DISTRIBUTION OF H$_\alpha$ EMISSION

We set up a scale sheet in front of the CCD camera before installation on ELISE. The distance of the scale sheet and the CCD camera is 52 cm which is equivalent to the center position of the ion source. Figure 3(a) shows the scale sheet image; focus condition and optical distortion is good enough to obtain a distribution. We confirm the proportional relationship of pixel number and distance as shown in Figure 3(b). The spatial distance per pixel corresponds to 0.0552 mm/pixel at the center of the source.

Figure 4(a) shows an typical output image for the wavelength of 656 nm taken by the spectrally-selective imaging system with 40 ms exposure time in hydrogen RF discharge at the shot number of 8788 in ELISE. The discharge power and filling gas pressure is 40 kW per driver and 0.6 Pa, respectively. Discharge area located 300 mm left from the LOS center which is outside of the image. Facing surface inside of vacuum vessel is illuminated by the reflected light from hydrogen plasma, but the circle area where is a hollow place of the opposite side viewing port becomes dark. The BP surface is located on the right side of the image between 850 and 1080 pixels; opening windows cutting in the BP around the beamlet groups looks like narrow slits. We superimpose the dotted circles for the angle θ from the center of LOS ($\theta = 2°$, $3°$, and $4°$). Viewing angle of $\theta = 4°$ is covered the area

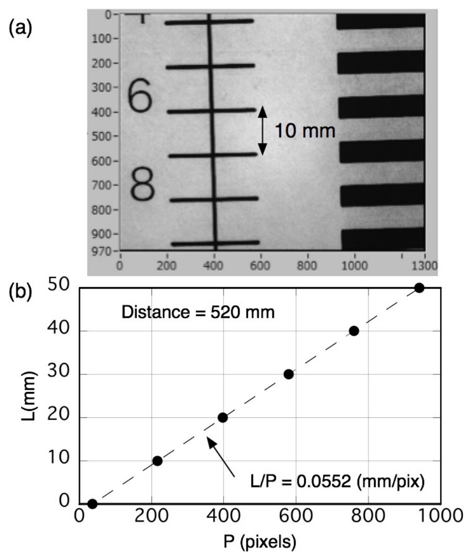

FIG. 3. (a) A scale sheet image located at 52 cm in front of the CCD camera. (b) Comparison of a pixel number and scale number, dashed line is the fitting line by linear function.

35 mm far from the LOS center. The central wavelength (λ_0) of the interference bandpath filter is sifted by the incident angle. Decrease value for λ_0 of the filter is 0.5 nm at the incident angle of 4°, which is negligible small to the 10 nm FWHM. Distribution measurement is not affected by difference of incident angle.

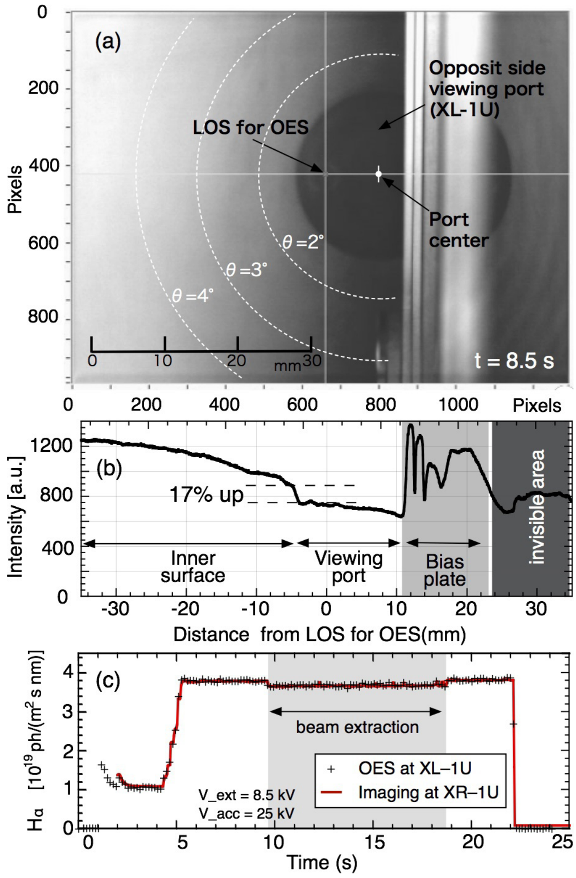

FIG. 4. (a) Photographic image for RF discharge taken by the imaging system at the XR−1U. (b)Horizontal distribution of H_α emission through the center of LOS. (c) Time traces of H_α intensity measured by the OES and imaging diagnostic at the same position.

Figure 4(b) shows the horizontal distribution of H_α emission through the center of LOS for imaging diagnostic. Horizontal axis is the distance from the position of OES port, which is converted by the value for spatial distance per pixel. Since an electron density and an ion density are high in the upstream side of the source, signal intensity of H_α emission gradually increase toward to the upstream direction. We find sharp signal increase at the boundary of viewing port due to increase of reflection signal from the inner surface. The signal contribution of reflection is 17%.

Figure 4(c) shows the time traces of H_α intensity measured by OES and imaging diagnostic at XL−1U and XR−1U, respectively. Time trend of the signal intensity of imaging measurement is good agreement with the OES signal. Therefore, the signal strength by the imaging measurement is possible to calibrate using a signal calibrated OES measurement. We find sudden signal reduction on H_α emission during beam extraction in both measurement. The cause of this reduction is not clear at present whether the main contribution is decrease of electrons or H^- ions in this discharge. To review details of its reduction on imaging diagnostic, a density measurement of negative ions and electrons will be needed at the same places and same discharge.

IV. CONCLUSION

A spectrally-selective imaging system has been performed well in the RF negative ion source in the ITER-relevant negative ion beam test facility ELISE. A distribution of H_α reductions are clearly observed in the multi-pulse operation. The time trend its intensity is consistent to the H_α intensity measured by OES at the same position. Therefore, signal intensity of image can be calibrated by calibrated OES measurement. The future direction of this study will be a identification of the relationship between a H_α emission intensity and a H^- density, that will contribute to optimize RF source performance for ELISE and ITER-NBI.

ACKNOWLEDGMENTS

We are grateful to the late Dr. P. Franzen whose supports and useful discussions were innumerably valuable throughout of this study. We also thanks technical staffs in IPP Garching for arrangement of diagnostic and ELISE operation. The authors acknowledge the financial support by SOKENDAI Young Researchers Overseas Visit Program to research in IPP Garching. This research is also supported by JSPS KAKENHI Grant Number 25249134, and the budget for the NIFS No. ULRR702 and No. ULRR009.

[1]K. Ikeda, H. Nakano, K. Tsumori, M. Kisaki, K. Nagaoka, M. Osakabe, Y. Takeiri, and O. Kaneko, New J. Phys. **15**, 1367 (2013).
[2]K. Ikeda, H. Nakano, K. Tsumori, M. Kisaki, K. Nagaoka, M. Osakabe, Y. Takeiri, and O. Kaneko, Rev. Sci. Instrum. **85**, 02A724 (2014).
[3]R. Hemsworth, H. Decamps, J. Graceffa, B. Schunke, M. Tanaka, M. Dremel, A. Tanga, H. D. Esch, F. Geli, J. Milnes, T. Inoue, D. Marcuzzi, P. Sonato, and P. Zaccaria, Nucl. Fusion **49**, 045006 (2009).
[4]B. Heinemann, H. D. Falter, U. Fantz, P. Franzen, M. Froeschle, W. Kraus, C. Martens, R. Nocentini, R. Riedl, E. Speth, and A. Staebler, Fusion Eng. Des. **86**, 768 (2011).
[5]P. Franzen, D. Wünderlich, R. Riedl, R. Nocentini, F. Bonomo, U. Fantz, M. Fröschle, B. Heinemann, C. Martens, W. Kraus, A. Pimazzoni, and B. Ruf, AIP Conf. Proc. **1655**, 060001 (2015).
[6]D. Wünderlich, U. Fantz, P. Franzen, R. Riedl, and F. Bonomo, Rev. Sci. Instrum. **84**, 093102 (2013).